



Isı Bilimi ve Tekniği Dergisi

Archive: <https://tibtd.org.tr/dergi>

A comparative study on the applicability of the solar energy-powered embedded pipe envelope system in different envelope locations

Linfeng WANG ¹, Chiu Chuen ONN ^{1, *}, Bee Teng CHEW ², Wuyan LI ³ and Yongcai LI ⁴¹ Department of Civil Engineering, Faculty of Engineering, Universiti Malaya, Lembah Pantai, Kuala Lumpur 50603, Malaysia² Department of Mechanical Engineering, Faculty of Engineering, Universiti Malaya, Lembah Pantai, Kuala Lumpur 50603, Malaysia³ Yunnan Key Laboratory of Disaster Reduction in Civil Engineering, Faculty of Civil Engineering and Mechanics Kunming University of Science and Technology, Kunming 650500, China⁴ School of Civil Engineering, Chongqing University Chongqing 400045, China

ARTICLE INFO

2025, vol. 45, no.2, pp. 162-171

©2025 TIBTD Online.

doi: 10.47480/isibted.1618182

Research Article

Received: 16 January 2025

Accepted: 11 July 2025

* Corresponding Author

e-mail: onnchiuchuen@um.edu.my

Keywords:

Solar thermal collector
Pipe embedded envelope
Building envelope applicability
Thermal performance
TRNSYS

ORCID Numbers in author order:

0009-0002-0419-1871

0000-0002-5093-5651

0000-0002-2101-9638

0009-0004-9514-1160

0000-0002-2027-9534

ABSTRACT

This study compares the heating efficiency of the Solar Energy-powered Embedded Pipe Envelope System (SEPES) in various building envelope locations using a novel simulation model developed with TRNSYS. The evaluation includes indoor air temperature, inlet and outlet water temperatures in walls, internal surface temperatures of envelopes, and heating energy consumption across six different SEPES installations. Key findings include: 1) SEPES significantly improves indoor temperatures during cold winters in Harbin, with ceiling installations increasing temperatures by up to 8.4°C, and strategic placements optimizing warmth and energy efficiency; 2) Water temperature in SEPES pipes indicates heating capacity, with the highest temperatures in east and west wall installations; 3) Ceiling-embedded pipes perform best in blocking heat loss, with surface temperatures ranging from 7.42°C to 11.59°C; 4) SEPES installations significantly reduce daily heat loads, with ceiling installations achieving the highest energy-saving rate of 49.7% and an 8.9-year payback period. 5) Installing SEPES in as many building envelope structures as possible can maximize the use of solar radiation to resist thermal insulation loads.

Farklı yapı kabuğu konumlarında güneş enerjisiyle çalışan gömülü borulu kabuk sisteminin uygulanabilirliği üzerine karşılaştırmalı bir çalışma

MAKALE BİLGİSİ

Anahtar Kelimeler:

Güneş termal kollektör
Boru gömülü yapı kabuğu
Yapı kabuğu uygulanabilirliği
Isıl performans
TRNSYS

ÖZET

Bu çalışma, TRNSYS yazılımı kullanılarak geliştirilen yeni bir simülasyon modeli aracılığıyla Güneş Enerjisiyle Çalışan Gömülü Borulu Kabuk Sistemi'nin (SEPES) farklı yapı kabuğu konumlarındaki ısıtma verimliliğini karşılaştırmaktadır. Değerlendirme kapsamında; iç ortam hava sıcaklığı, duvarlardaki giriş ve çıkış su sıcaklıkları, yapı kabuğunun iç yüzey sıcaklıkları ve altı farklı SEPES kurulumu için ısıtma enerjisi tüketimi incelenmiştir. Başlıca bulgular şunlardır: 1) SEPES, Harbin'deki soğuk kış koşullarında iç ortam sıcaklıklarını önemli ölçüde artırmaktadır. Tavan uygulamaları sıcaklığı 8.4°C'ye kadar yükseltirken, stratejik yerleşimler konforu ve enerji verimliliğini optimize etmektedir. 2) SEPES borularındaki su sıcaklığı, sistemin ısıtma kapasitesini göstermektedir; en yüksek sıcaklıklar doğu ve batı duvarı kurulumlarında elde edilmiştir. 3) Tavana gömülü borulu sistemler, ısı kaybını en iyi şekilde engellemiş ve yüzey sıcaklıkları 7.42°C ile 11.59°C arasında değişmiştir. 4) SEPES uygulamaları günlük ısı yüklerini önemli ölçüde azaltmıştır; tavan kurulumları %49.7'ye varan enerji tasarrufu oranı ve 8.9 yıllık geri ödeme süresi sağlamıştır. 5) SEPES'in mümkün olduğunca çok sayıda yapı kabuğu bileşenine entegre edilmesi, güneş radyasyonundan azami ölçüde yararlanarak ısı yalıtım yüklerine karşı direnç kazandırmaktadır.

NOMENCLATURE

CNY	Chinese Yuan
CHTC	Convective Heat Transfer Coefficient
HVAC	Heating, Ventilation, and Air Conditioning

PE-PCM	pipe-embedded phase change material
SEPEs	solar energy-powered embedded pipe envelope system
TRNSYS	Transient System Simulation Tool

INTRODUCTION

The Paris Agreement has established a global consensus on the necessity for energy conservation and low-carbon development. To further decrease energy consumption and carbon emissions, China aims to reach peak carbon dioxide emissions before 2030 and intends to achieve carbon neutrality by 2060 (Chen et al., 2020). In this context, the development of efficient energy-saving strategies and the enhancement of energy utilization efficiency hold substantial economic and environmental importance. At present, energy consumption in buildings constitutes a significant share of total societal energy consumption. In 2018, China's annual building energy consumption reached 1.123 billion tons of standard coal, resulting in almost 2.2 billion tons of CO_2 emissions (Guo et al., 2021). As living standards improve, there is a concomitant increase in the demand for indoor environmental quality in buildings. This has led to a significant surge in the energy consumption of building HVAC systems. Studies have shown that heating and air conditioning consume 50-60% of the total energy used in buildings in northern China (Yi, 2005). In regions with hot summers and cold winters, this figure increases to 65% (Yang, 2014). Consequently, lowering HVAC energy consumption in buildings is an essential approach to enhancing energy efficiency and reducing carbon emissions.

The building enclosure structure represents the boundary between the interior and exterior environments, and the heat transfer through this envelope is of significant importance in determining the building's heating and cooling load. In winter, the heat transfer loss of the enclosure structure is such that it exceeds 70% of the total heating load of the building (Li & Chen, 2019). Improving the thermal performance of a building plays an important role in reducing energy consumption associated with heating and air conditioning. Nevertheless, with the ongoing enhancement of the enclosure structure's performance, the potential for further enhancing its insulation and airtightness in reducing the energy consumption of heating and air conditioning has become increasingly constrained. The construction of thick walls represents a significant investment of valuable building space, which in turn increases the overall costs of construction. Furthermore, the incorporation of thick walls into a building design introduces an increased risk of fire safety hazards (Shen et al., 2017; Yang et al., 2021). Conversely, excessive insulation performance of the enclosure can result in an increased cooling load during the transition season and summer, thereby increasing air conditioning energy consumption (D'Antoni & Saro, 2013). In this context, the exploration of active control methods for enclosure structures has attracted the attention of researchers.

The embedded pipe envelope represents a novel enclosure structure that integrates a circulating pipeline system. The circulation of a heated or cooled medium within the pipes effectively intercepts heat or cold loss through the envelope, thereby providing a novel solution to the challenge of thermal energy loss in building enclosures (Xie et al., 2012; Xu et al., 2010). As one type of the thermal active building system, embedded pipe envelope could be coupled with different cooling and heating sources (Jiang et al., 2020; Jobli et al., 2019;

Krzaczek et al., 2019; Sun et al., 2020). The ground source heat pump is employed by Li to provide the heat required for winter heating to the embedded pipe wall (Shen & Li, 2017; Shen et al., 2017). The findings of the analysis indicate that the application of hot water at temperatures below room temperature can also be employed as an auxiliary heating source for residential buildings. During the heating season in Beijing, the system is capable of reducing the heat load by up to 84%, while the heat loss on the outer wall only increases by 18%. The energy-saving rate of the entire system is 44%, and the investment payback period is 2 years. Peizheng Ma (Ma et al., 2014) conducted a model of hydronic radiant cooling building using a parametric cooling tower in one summer in seven U.S. cities. They suggested that a pipe-embedded envelope with a cooling tower is only viable in regions with specific mesoscale climatic conditions, such as Sacramento, CA. In other areas, the coupling system can only achieve partial homeostasis. Krzaczek et al. (Krzaczek & Kowalczyk, 2011) proposed a method of directly heating residential buildings using solar energy as a heat source. This method involves embedding polypropylene U-shaped pipes inside the exterior wall, allowing fluid to flow within the U-shaped pipe system with variable flow rates and inlet temperatures. The efficacy of this method in maintaining wall temperature stability during cold seasons has been demonstrated through empirical research. The unpredictable and intermittent characteristics of solar radiation can be effectively managed by integrating it with building structures possessing significant thermal mass. This integration occurs simultaneously with the circulation of heat transfer mediums within solar collectors. This integration allows for the successful coupling of solar collectors with pipe-embedded envelopes, which exhibit a high response time. This integration is further supported by the fact that solar thermal system could be coupled with embedded pipe envelopes.

When coupled with a solar thermal collector, the pipe of the system can be embedded into different building envelopes, thereby contributing to the heating capacity of the indoor space, typically in the form of walls (He et al., 2022; Shen et al., 2022) (Yang & Chen, 2024), floors (Feng et al., 2016), or ceilings (Su et al., 2019; Ye et al., 2021). The specific geographical location and area of pipe embedded envelope has a considerable effect on the investment cost and thermal performance of the building. To avoid the higher energy consumption caused by the unequal heat gain from the solar radiation in south and north wall, Junhao Shen etc. (Shen et al., 2022) put forth the concept of an active pipe embedded system with the objective of achieving heat redistribution between the north and south walls. The findings indicated that in an environment characterized by elevated temperatures during the summer months and reduced temperatures during the winter months, rooms utilizing the system exhibited a 12.8% reduction in heating requirements during the designated heating season, in comparison to the control rooms. For cold climate, the heating loads in January is reduced by 8.7%. Jinjuan (Feng et al., 2016) proposed a streamlined approach to optimizing radiant floor design through the utilization of solar radiation. Their findings indicated that in scenarios with direct solar exposure, the system's capacity could potentially increase by up to $130-140W/m^2$. Kan Xu (Xu et al., 2023) put forth an

innovative roof design that integrates a pipe-embedded phase change material (PE-PCM) with a solar thermal collector. The objective is to enhance the utilization of solar energy and improve the overall efficiency of the building. To this end, the PE-PCM layer is positioned on the interior side of the roof. Their findings revealed that this novel structure effectively meets heating demands, reducing energy consumption for indoor heating by 53% compared to a traditional roof design.

As previously discussed, the solar energy-powered embedded pipe envelope system (SEPES) is an effective solution for reducing indoor heating loads and enhancing thermal comfort. The author's existing research (Wang et al., 2024) indicates that the SEPES has the potential to increase the indoor temperature by 14.4°C on the coldest heating day in a rural building in Beijing. Regional adaptability studies further demonstrate that SEPES performs well across various regions and is particularly effective in climates with low temperatures and ample solar radiation. Regarding the aforementioned literature, SEPES can be coupled with different envelope locations, such as floor, wall and ceiling. Due to the different orientations of the received solar radiation and the boundary conditions, the performance of building envelope structures coupled with SEPES varies. Hence, investigating the thermal performance of SEPES when activated in different envelope locations is of significance. In this research, the thermal performance of SEPES coupled with six different envelope locations was systematically evaluated, including indoor air temperature, Inlet and outlet water temperature in the wall, internal surface temperature of envelopes and heating energy consumption. The findings of this study are anticipated to provide valuable insights into the practical implementation of SEPES, enhancing its applicability in real-world scenarios.

SYSTEM OVERVIEW AND NUMERICAL MODELING

The configuration of SEPES

The configuration of SEPES is illustrated in Figure 1. This system comprises solar collectors, a thermal storage tank, and embedded pipes integrated into the building's exterior walls. These walls are constructed with a brick layer, and the water pipes are positioned centrally within the walls in a serpentine pattern. The pipe-embedded structure covers areas equivalent to the corresponding solid wall areas, with the embedded pipe surface areas measuring 11.25m², 13.5m², 26.28m², and 11.46m² for the eastern, western, northern, and southern walls, respectively. Heat is transferred through the water in the pipes to the facades of the building in sequence, facilitated by a water pump that drives the circulation throughout the system.

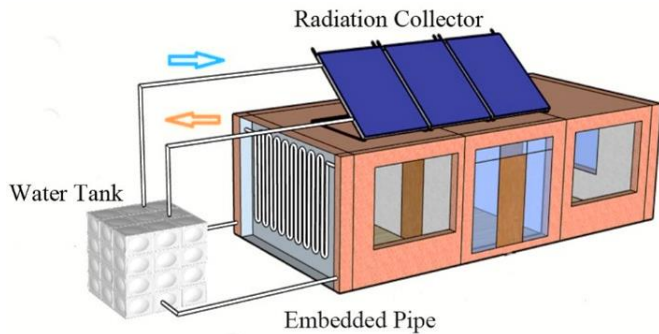


Fig. 1 The configuration of SEPES

The heat storage tank comprises two distinct circulating water loops. As previously indicated, the initial loop is situated within the pipe-embedded walls. In the second loop, the heat

generated by the photothermal effect is transferred to a thermal storage water tank, where it is stored and then transferred to the building envelope. The solar thermal collector, situated on the roof, comprises a high-absorptance surface that absorbs solar radiation, thereby generating heat, which is subsequently employed to warm the circulating water within the system.

Model setting

The numerical simulating model for this study was built in TRNSYS software (shown in Fig. 2). The model comprises components and functions, which are mainly delineated in Table 1.

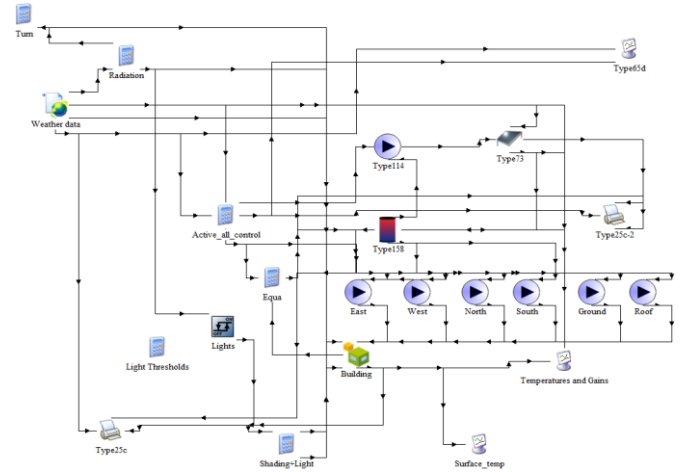


Fig. 2 Simulation model of SEPES

The SEPES is particularly well-suited to standalone buildings due to the innovative structural design. The case study presented in this study is a typical rural building located in Harbin, a northern city of China, as illustrated in Figure 3. The building envelope design characteristics comply with design standards for cold regions in China. The building, oriented to the south, is a representative rural dwelling with a population density of 0.05 persons/m². The solar absorption and emissivity values of all windows are 0.60 and 0.90 respectively. The SEPES is designed with a solar collector in series with a total area of 80 m², the absorber plate absorptance of 0.90 and the fluid specific heat capacity of 4.19 kJ/(kg · K). The system includes a 10 m³ water tank with a heat loss coefficient of 3.4 kJ/(h · m² · K). To ensure effective circulation, six pumps, each rated at 180 W and with a flow rate of 500 kg/h, are arranged in a series, supplemented by a 100 W system pump to maintain overall fluid movement. Additional building information can be found in Table 2.

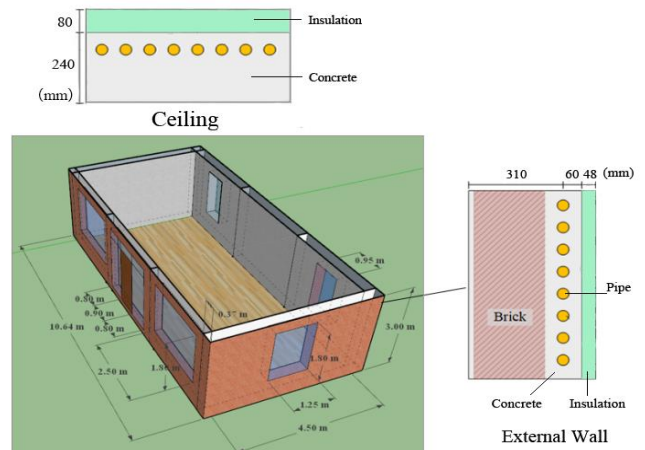


Fig. 3 The typical building in this research

Table 1. The function of components in TRNSYS.

Component Name	Number	Function
Solar thermal collector	Type 73	This model simulates the thermal performance of an idealized flat-plate collector.
Water pump	Type 114	The model depicts a single pump operating at a constant speed, designed to sustain a consistent fluid outlet mass flow rate.
Water Tank	Type 158	The model depicts a storage tank with a constant volume, filled with fluid.
Weather data	Weather data	This component supplies data on outdoor temperature and humidity, while also calculating solar radiation.
Outputs	Type 65d	This component output the calculation results of other components.
Printer	Type 25c	This component output selected system variables at specified intervals of time
Differential Controller	Type 165	This component generates a control function with a value of either 1 or 0.

Table 2. Thermo-physical parameters of the building enclosure structure.

	Material Layers		CHTC ($w/(m^2 \cdot K)$)		U-Value ($w/(m^2 \cdot K)$)
	Name	Thickness (mm)	Interior	Lateral	
External Wall	Brick	370 (E, W, N) 240 (S)	3.06	17.78	0.6 (E, W, N) 0.65 (S)
	Concrete	120			
	Insulation	48			
Floor and Interior walls	Insulation	30	3.06	3.06	1.0
	Concrete	120			
Roof	Insulation	80	3.06	17.78	0.45
	Concrete	240			
External window	Glass	4	3.06	17.78	3.2
	Air	3.2			
	Glass	4			

*CHTC means Convective Heat Transfer Coefficient.

RESULTS AND DISCUSSION

The northern regions of China have both centralized and non-centralized heating periods through the year. The central heating period in Harbin is from 20 October to 20 April of the following year, approximately 180 days, or half the year. Figure 4 presents a visual representation of the annual variations in outdoor and naturally occurring indoor temperatures of rural buildings within the Harbin region. As shown in the figure, due to the attenuating and delaying effect of the building envelope structure on solar radiation and outdoor temperature changes, the indoor air temperature fluctuation is smoother than the outdoor, and the average annual indoor temperature is about 2.5 °C higher than the outdoor temperature. However, throughout the period of heating, the temperature of the indoor air is, in the majority of cases, below 10 °C, with approximately half of all instances occur below 0 °C. As a result, the case building has a significant heating requirement during the heating season.

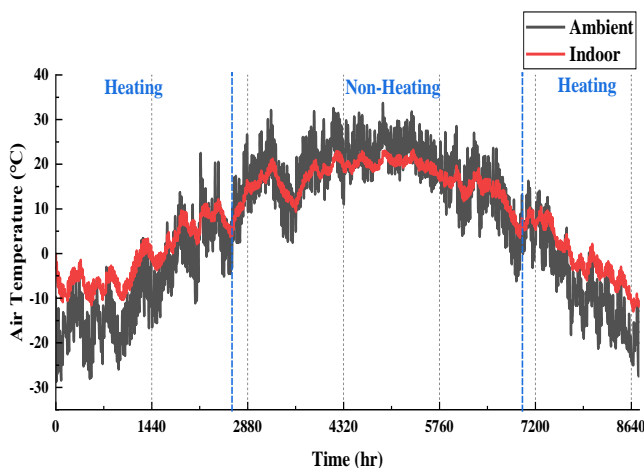


Fig. 4 Annual ambient air temperature and natural indoor air temperature of the case building in Harbin

Thermal performance on a typical heating day

Indoor air temperature

The indoor air temperature of the buildings in this study is significantly affected by the outdoor low temperature environment during the heating season. Figure 5 illustrates the trend of indoor air temperature changes when pipes are embedded in different building envelope locations. As shown in the Figure, for a typical heating day (2nd January) in Harbin, the outdoor air temperature variation range is -27°C to -12.3°C, with an average temperature of -20°C. For a raw building without SEPES, due to the barrier of the building envelope structure and the influence of indoor heat sources, the fluctuation range of indoor air temperature is relatively small, ranging from -8.6 °C to -5.2 °C. The sunshine duration in Harbin on January 2nd is about 8 hours. The application of the SEPES system in the building has a very positive effect on the thermal environment in the building. The embedding of pipes in any part of a building's enclosure structure can have the effect of raising the indoor air temperature for 24 hours. The implementation of the SEPES has been observed to result in a notable increase in the maximum air temperature in the room, reaching 1.8°C when the pipe is embedded in the floor. This represents a significant rise of 7°C compared to the scenario without SEPES. Here the SEPES works in a similar way to a floor radiant system, which can transfer most of the heat provided by the sun to the indoor environment. Due to the presence of solar collectors, the ceiling is the least exposed to direct sunlight. When SEPES works in the ceiling, the ceiling is the enclosure structure that offers the most resistance to heat loss. with the maximum increase being 8.4°C. Among the four walls, the north wall receives the least amount of direct sunlight and has the lowest wall temperature. Therefore, more heat is lost from the north wall to the ambient. When SEPES is installed on the north wall, it can significantly increase indoor air temperature. On average, there is an increase of 6.1°C per day, with a maximum increase of 6.2 °C. SEPES installed on the south wall can increase the average air temperature in the room by 4.4°C, and SEPES installed on the east and west walls can increase the temperature by 3.2°C. The results of the

analysis indicate that the installation of SEPES in the ceiling has a more pronounced effect on the improvement of the indoor air temperature, while the installation of SEPES on the west and east walls has a less significant impact. If SEPES is mainly installed in walls to isolate insulation loads, it is recommended to set it in the north wall. The heat storage tank can maintain the heating capacity of the system for 24 hours.

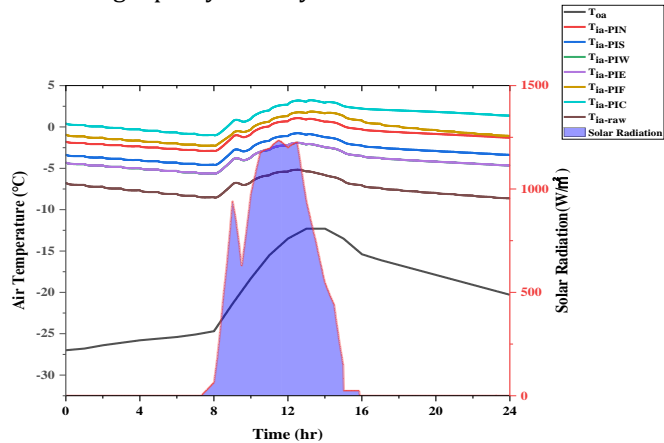


Fig. 5 Trend of indoor air temperature changes when pipes are embedded in different building envelope locations.

Further analysis of the combined installation configuration reveals enhanced thermal performance when SEPES is simultaneously deployed on both the ceiling and north wall (Figure 6). For the same typical heating day in Harbin, this dual-configuration achieves a maximum indoor air temperature of 4.24°C (surpassing individual ceiling/north wall installations by 1.84°C/2.44°C respectively) and maintains an average temperature of 2.1°C throughout the day. Notably, the system demonstrates effective temperature stabilization, with the lowest recorded temperature being 0.4°C - significantly higher than the -8.6°C of the untreated building. Compared to single-sided applications, the installation of SEPES on all building surfaces (ceiling, floor, and four walls) shows significantly enhanced thermal performance, with a maximum indoor temperature of 7.56 °C, a minimum temperature of 3.32 °C, and an average temperature of 5.3 °C. This means an increase of 4.15 °C compared to the average temperature of only installing the ceiling (average 1.15 °C). The significant improvement in performance comes from the collaborative thermal regulation of multiple surfaces and the elimination of thermal bridges. Although SEPES can be selectively installed on the ceiling or north wall when considering cost-effectiveness or construction convenience, installing SEPES in as many building envelope structures as possible can maximize the use of solar radiation to resist thermal insulation loads.

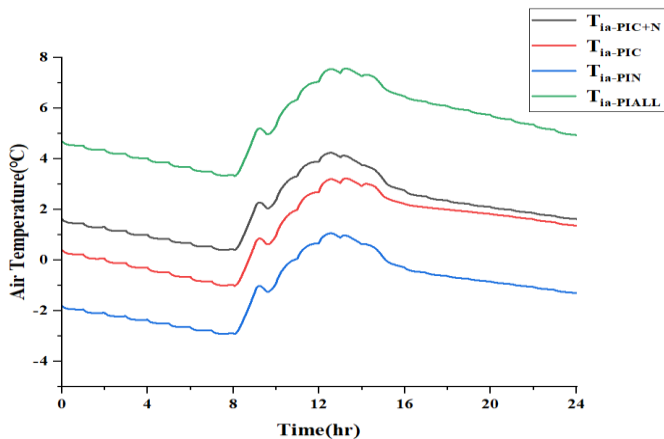
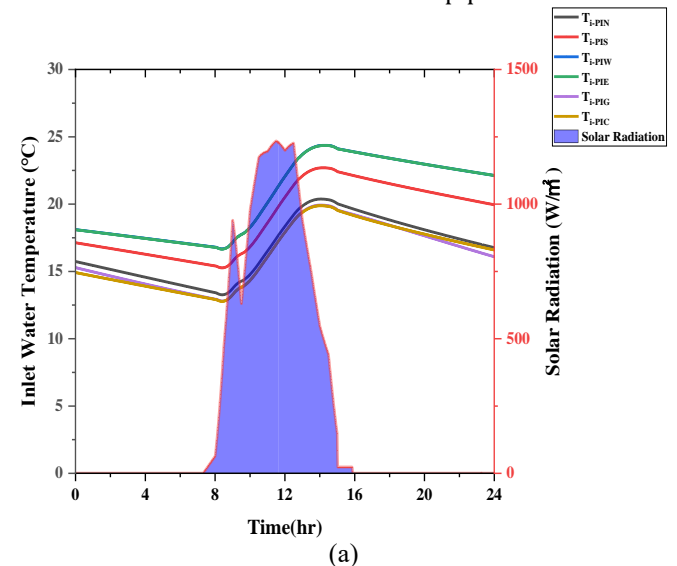
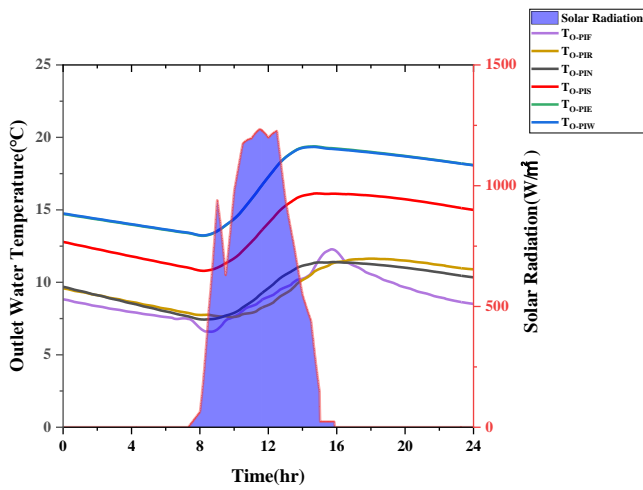


Fig. 6 Comparison of indoor air temperature variations for SEPES installed on ceiling only, north wall only, combined ceiling-north wall and combined all envelopes configuration

Inlet and outlet water temperature in the wall with the SEPES

The variation in water temperature within the pipes embedded in the envelopes can indicate the heating capacity of the SEPES system for the building, as well as its ability to manage the heat load. Figure 6 illustrates the inlet and outlet water temperatures of the SEPES installed in different envelope locations. The research building is in the northern hemisphere and faces south. The thermal performance of SEPES pipes installed on the east and west walls of the building is almost the same. As shown in the figure, the inlet water temperature of the SEPES pipes embedded in the east and west walls is the highest, ranging from 16.7°C to 24.4°C daily, with an average temperature of 20.6°C. The outlet water temperature of the SEPES pipes embedded in the east and west walls is the highest, with a daily range of 13.2°C to 19.4°C and an average temperature of 16.5°C. The average temperature difference between the inlet and outlet of the pipes is 4.1°C. The smaller area of the east and west walls relative to other envelopes results in less heat loss, which reduces the potential for indoor and outdoor heat dissipation. Additionally, the ceiling is obstructed by a solar collector, preventing the direct radiation of solar energy from the sun and the long-wave radiation from the sky to the collector, which results in a loss of heat. When the SEPES pipe is embedded in the ceiling and floor, the water temperature is relatively lower than when installed in the other 4 positions. The average temperature of inlet and outlet water is only 16.2 °C and 9.6 °C respectively, with a difference of 6.6°C. Moreover, a comparison of the water temperature at the embedded pipe inlet and outlet on the south wall of the SEPES-installed building with those on the corresponding north wall revealed that the south-wall inlet and outlet exhibited a higher temperature. The maximum values of the inlet and outlet water temperatures of the south wall are 22.7°C and 16.2°C, respectively, while the corresponding temperatures of the north wall are 20.4°C and 11.5°C. Furthermore, there is a delay of about 3 hours between the fluctuation of water temperature in the SEPES storage tank and the fluctuation of solar radiation intensity. This is primarily a result of the heat storage capacity and thermal resistance of the building envelopes. In conclusion, the temperature of the water within the pipe represents the effective temperature of the SEPES. The variation in the effective temperature of the SEPES is primarily influenced by direct solar radiation and the surface area of the embedded pipe walls.



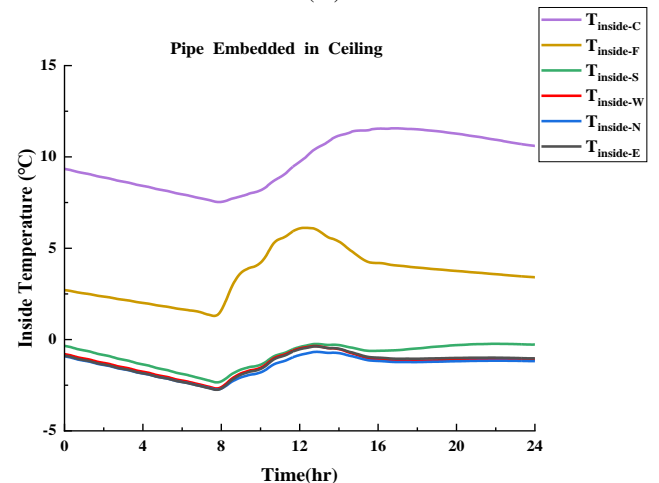
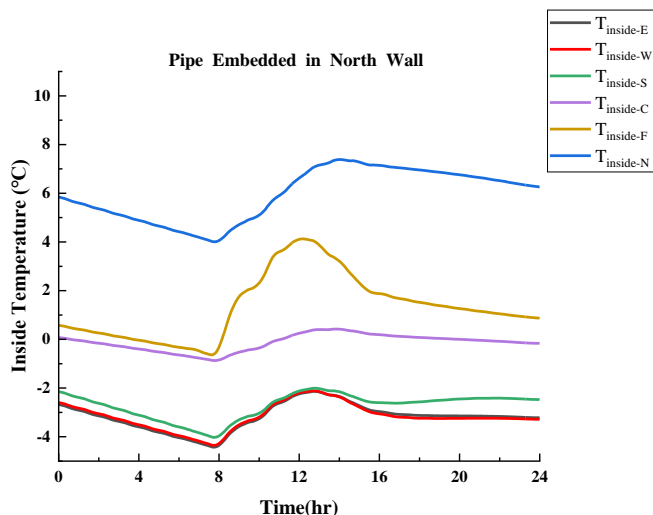
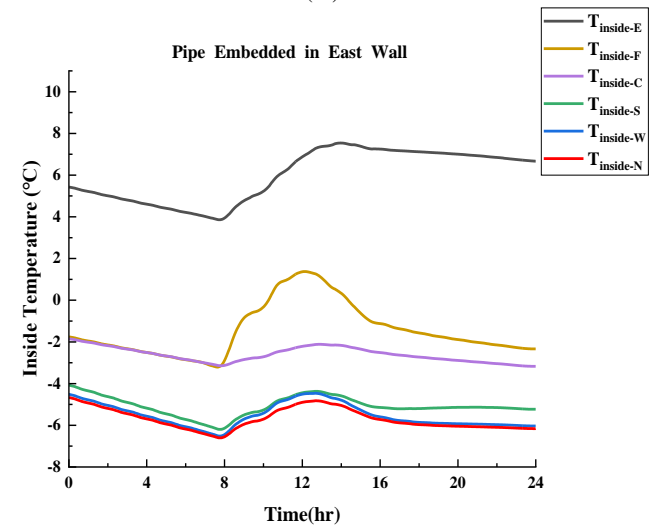
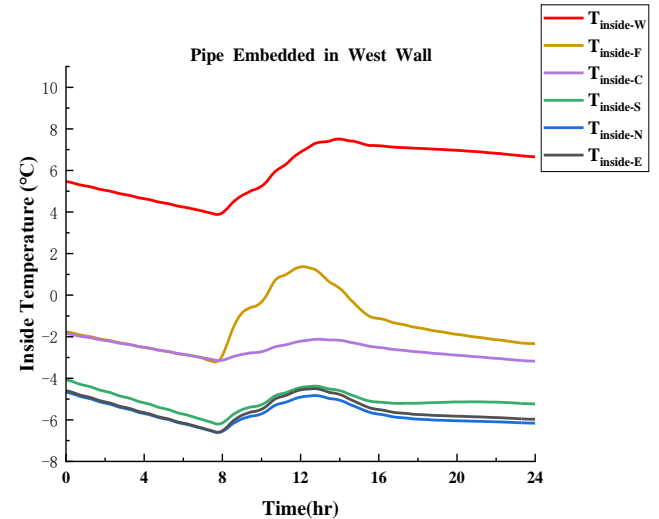
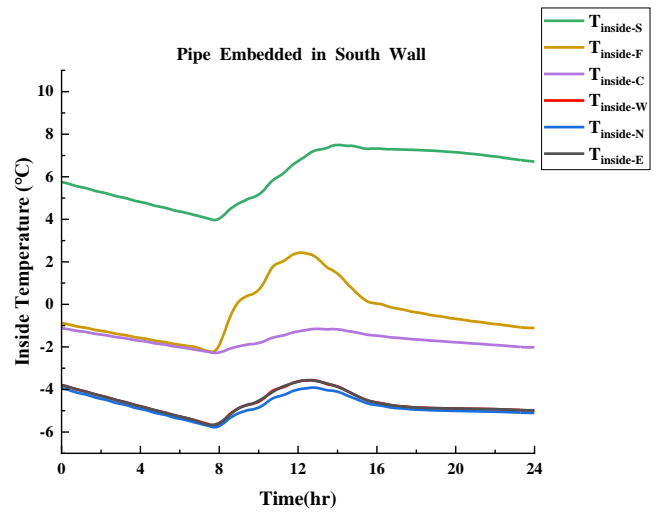


(b)

Fig. 7 (a) Inlet water temperature in the wall with the SEPES; (b) Outlet water temperature in the wall with the SEPES.

Internal surface temperature of the envelopes

The inner surface of the building envelope undergoes convective heat exchange with the indoor air and radiative heat exchange with occupants and objects, both of which influence the thermal comfort of the indoor environment. The temperature of all walls, ceiling, and floor when SEPES pipes are embedded into different building envelope structures is presented in Figure 8. The internal surface temperature of the envelope, which contains embedded pipes, is demonstrably higher than that of other surfaces. As previously stated, the pipe embedded in ceiling exhibits superior heat load blocking capability. Upon pipe integration into the ceiling, the temperature range of the inner surface of the ceiling exhibits fluctuations between 7.42 °C and 11.59 °C. The daily average temperature of the inner surface of the building envelopes is as high as 1.39 °C. The absence of direct contact between the floor and outdoor air results in a reduction in heat loss. Even in the absence of solar radiation, the maximum internal surface temperature of the floor can reach 11.3 °C. In this instance, the mean daily temperature on the internal surface of the building envelope is recorded at -0.12 °C. Moreover, the mean temperature of the inner surface of the envelope when the pipeline is situated within the eastern, western, southern, and northern walls is -2.4 °C, -2.4 °C, -1.7 °C, and -0.3 °C, respectively. The preceding analysis demonstrates that the installation position of SEPES has a considerable influence on the overall heat loss of the building.



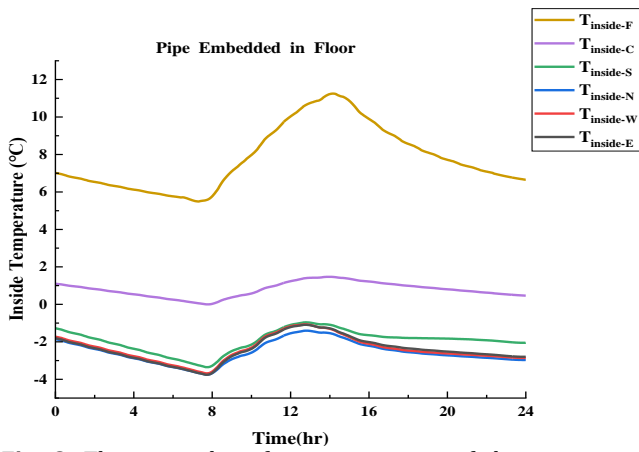
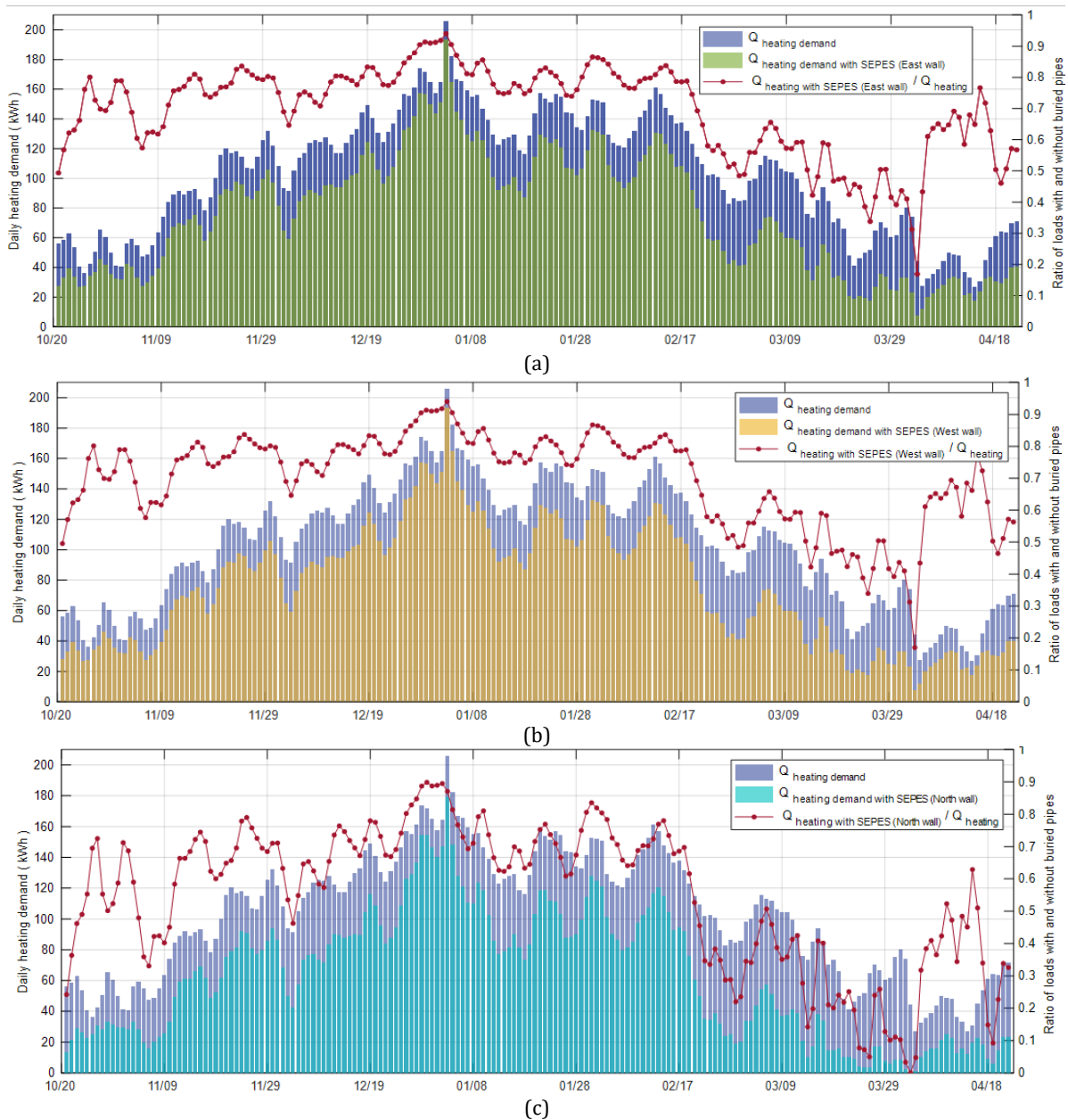


Fig. 8. The internal surface temperature of the various pipe embedded building envelopes.

Energy saving in heating period

As previously stated, the SEPES, which is one of the thermal active building systems, has the capacity to reduce the heat load during the heating period of the building. In order to evaluate the energy-saving effectiveness of SEPES installations in different enclosure structures for heating, a comparative

analysis was conducted of the daily heating loads across six installation positions. As demonstrated in Figure 9, following the activation of the SEPES system, the daily heat load of buildings during the heating season is reduced to varying degrees. When the SEPES is active in different envelope locations, the average daily heat load through heating season ranges from $53.31 kWh/D$ to $76.69 kWh/D$, while the average daily heat load of the case building is $103.8 kWh/D$ without SEPES. Following the incorporation of SEPES into the ceiling, the total heating load for the season was observed to decrease from the initial $18,897.06 kWh$ to $9,702.42 kWh$, resulting in an energy-saving rate of 49.7%. This represents the most significant energy-saving effect compared with other positions. Moreover, as shown in Figure 9(f), during some periods in March and April, the heat load can even be completely compensated by SEPES. In addition, compared to the other three walls, the maximum heat load reduction is achieved when SEPES is installed on the north wall. The average daily heat load is $64.03 kWh/D$ and energy-saving rate is 44% in this condition. Overall, the best thermal performance is achieved when the SEPES is installed in the ceiling. For other envelopes, the ability to reduce the consumption of heating energy is classified from the largest to the smallest as the north wall, the floor, the south wall, the east wall and the west wall.



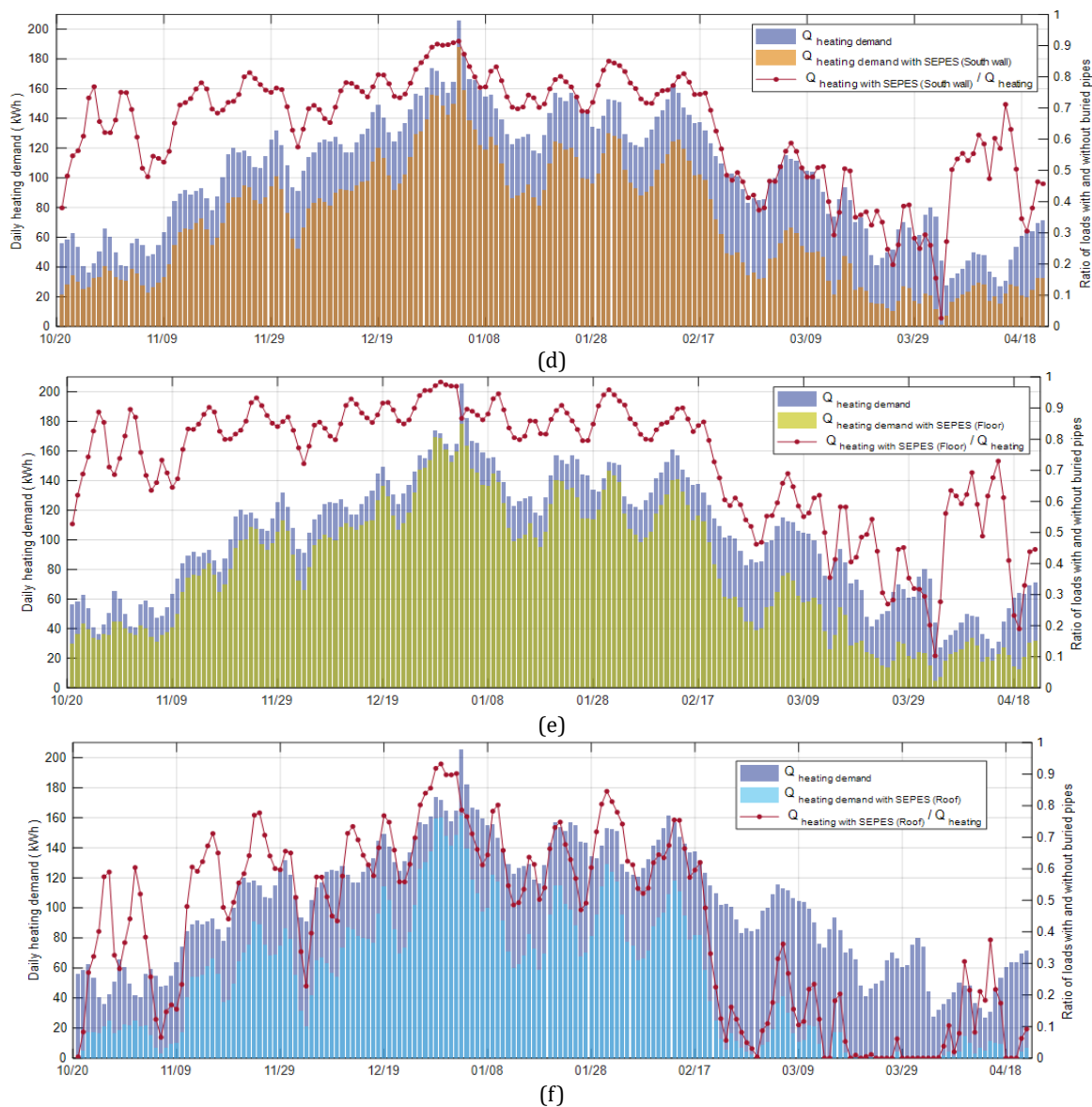


Fig. 8 Heating energy consumption of SEPES when pipe is embedded in different envelope locations: (a) East wall; (b) West wall; (c) North wall; (d) South wall; (e) Floor; (f) Ceiling.

Payback period for ceiling-installed SEPES

Based on the previous analysis results, the investment payback period analysis of the SEPES system installed on the ceiling is selected to verify its economic feasibility as a sustainable heating solution. As shown in Table 3 and Table 4, the initial total investment of the system is 19500 CNY, including a solar collector system (10 square meter flat plate collector 6300 CNY), embedded PEX pipe structure (48 square meters 4800 CNY), a water tank (6000 CNY), pumping system (two 180W units 400 CNY), and control components (2000 CNY), which can save a large amount of energy of 9194.64 kWh/year. Calculated based on a gas centralized heating efficiency of 0.7, the price is 0.45 CNY/kWh, which is equivalent to saving 4137.6 CNY in energy costs annually. After deducting 195 CNY in maintenance costs (1% of the initial investment), the net annual savings are 2187.6 CNY. These numbers result in a calculated investment payback period of 8.9 years, indicating strong financial feasibility of the system in cold climate applications. The SEPES system could be designed with durable materials, including PEX piping (30+ year lifespan) and corrosion-resistant solar collectors (20–25 years). Regular maintenance (e.g., pump replacements every 10 years) ensures operational longevity. Given the system's expected lifetime of 25–30 years, the 8.9-year payback period represents only 30% of its service life, leaving ample time for net positive

returns. This economic performance complements the proven thermal benefits of the system, as mentioned in previous sections. The investment return period of 8.9 years is within an acceptable range for building energy renovation projects. Further improvement in the calculation of investment payback period can incorporate factors such as expected energy price increases and potential system performance decline over time.

Table 3. Initial cost of the ceiling-installed SEPES

Calculation Component	Parameter Description	Unit Number	Value
Initial Investment			
Solar Collector System	-Type: Flat plate	10m ²	6300 CNY
	-Unit Cost: 600 CNY/m ²		
Embedded Pipe Structure	-Installation: 5% of equipment cost	48m ²	4800 CNY
	Pipe material: PEX		
Water tank	-Construction cost: 100CNY/m ²	1	6000 CNY
	-Volume: 10 m ³		
Pump	-Power rate: 180 W	2	400 CNY
	-unit price: 200 CNY		
Control system and other components	Valves, Control system, Pipes	1	2000 CNY
Total Initial Investment			19500 CNY

Table 4. Annual Savings and Payback Period Analysis of the SEPES System

Annual Savings	
Energy Saved	9194.64 <i>kWh</i>
Energy Price	0.45 CNY/ <i>kWh</i>
	1% of initial investment: 1950 CNY
Net Annual Savings	2187.6 CNY
Payback Period	8.9 years

CONCLUSIONS

To compare the heating efficiency of the solar energy-powered embedded pipe envelope system in different building envelope, this study developed a novel simulation model by coupled building with SEPES through TRNSYS. The indoor air temperature, Inlet and outlet water temperature in the wall, internal surface temperature of envelopes and heating energy consumption of SEPES coupled with six different envelope locations was systematically evaluated. In summary, the conclusions can be drawn as follows:

(1) The SEPES significantly improves indoor temperatures during cold winters in Harbin. Embedding SEPES in the ceiling is particularly effective, increasing indoor temperatures by up to 8.4°C, while installations on the walls also contribute but to a lesser extent. Although SEPES can be selectively installed on the ceiling or north wall when considering cost-effectiveness or construction convenience, installing SEPES in as many building envelope structures as possible can maximize the use of solar radiation to resist thermal insulation loads.

(2) The study demonstrates that the water temperature in the SEPES pipes effectively indicates the system's heating capacity and heat load resistance. The SEPES pipes located within the east and west walls exhibited the highest inlet and outlet water temperatures, with average values of 20.6°C and 16.5°C, respectively. This is attributed to the reduced heat loss from these smaller walls. Conversely, pipes located in the ceiling and floor exhibit lower temperatures, with an average of 16.2 °C at the inlet and 9.6 °C at the outlet. This is due to obstructions and reduced solar radiation. The south wall exhibits higher temperatures than the north wall, which highlights the impact of direct solar radiation and the area of embedded pipes on the efficiency of the SEPES system.

(3) Ceiling-embedded pipes perform best, with temperatures ranging from 7.42°C to 11.59°C, effectively blocking heat loss. Floors also retain heat well, reaching up to 11.3°C even without solar radiation. The average inner surface temperatures for walls vary, with the north wall being the warmest at -0.3°C. These findings indicate that the position of SEPES installation greatly influences the building's overall heat loss and thermal performance.

(4) Comparative analysis indicates that the installation of SEPES significantly reduces the daily heat loads, with average reductions ranging from 53.31 *kWh/D* to 76.69 *kWh/D*, in comparison to 103.8 *kWh/D* without SEPES. The ceiling installation of SEPES yielded the highest energy-saving rate of 49.7%, reducing the total heating load from 18,897.06 *kWh* to 9,702.42 *kWh*. The north wall installation also demonstrates a notable reduction in energy consumption, with a 44% decrease. In terms of overall thermal performance, the ceiling installation is the most effective, followed by the north wall, floor, south wall, east wall, and west wall, in descending order

of efficacy. The ceiling-installed SEPES demonstrates strong economic viability, with an 8.9-year payback period.

ACKNOWLEDGEMENT

The authors are grateful for the financial support of the Research University (RU) Grant - Faculty Program (Grant No. GPF005A-2023) and the Chongqing Science and Technology Commission, China (No. CSTB2022NSCQ-MSX1019)

REFERENCES

- Chen, H., Yang, L., & Chen, W. (2020). Modelling national, provincial and city-level low-carbon energy transformation pathways. *Energy Policy*, 137, 111096. <https://doi.org/10.1016/j.enpol.2019.111096>
- D'Antoni, M., & Saro, O. (2013). Energy potential of a Massive Solar-Thermal Collector design in European climates. *Solar energy*, 93, 195-208. <https://doi.org/10.1016/j.solener.2013.04.011>
- Feng, J., Schiavon, S., & Bauman, F. (2016). New method for the design of radiant floor cooling systems with solar radiation. *Energy and Buildings*, 125, 9-18. <https://doi.org/10.1016/j.enbuild.2016.04.048>
- Guo, S., Yan, D., Hu, S., & Zhang, Y. (2021). Modelling building energy consumption in China under different future scenarios. *Energy*, 214, 119063. <https://doi.org/10.1016/j.energy.2020.119063>
- He, Y., Zhou, H., & Fahimi, F. (2022). Modeling and demand-based control of responsive building envelope with integrated thermal mass and active thermal insulations. *Energy and Buildings*, 276, 112495. <https://doi.org/10.1016/j.enbuild.2022.112495>
- Jiang, S., Li, X., Lyu, W., Wang, B., & Shi, W. (2020). Numerical investigation of the energy efficiency of a serial pipe-embedded external wall system considering water temperature changes in the pipeline. *Journal of Building Engineering*, 31, 101435. <https://doi.org/10.1016/j.jobbe.2020.101435>
- Jobli, M. I., Yao, R., Luo, Z., Shahrestani, M., Li, N., & Liu, H. (2019). Numerical and experimental studies of a Capillary-Tube embedded PCM component for improving indoor thermal environment. *Applied Thermal Engineering*, 148, 466-477. <https://doi.org/10.1016/j.applthermaleng.2018.10.041>
- Klein, S. A. (2018). Calculation of Flat-Plate Collector Loss Coefficients. *Renewable Energy*. <https://doi.org/10.4324/9781315793245-69>
- Krzaczek, M., Florczuk, J., & Tejchman, J. (2019). Improved energy management technique in pipe-embedded wall heating/cooling system in residential buildings. *Applied energy*, 254, 113711. <https://doi.org/10.1016/j.apenergy.2019.113711>
- Krzaczek, M., & Kowalczyk, Z. (2011). Thermal Barrier as a technique of indirect heating and cooling for residential buildings. *Energy and Buildings*, 43(4), 823-837. <https://doi.org/10.1016/j.enbuild.2010.12.002>

- Li, N., & Chen, Q. (2019). Experimental study on heat transfer characteristics of interior walls under partial-space heating mode in hot summer and cold winter zone in China. *Applied Thermal Engineering*, 162, 114264. <https://doi.org/10.1016/j.applthermaleng.2019.114264>
- Ma, P., Wang, L.-S., & Guo, N. (2014). Modeling of hydronic radiant cooling of a thermally homeostatic building using a parametric cooling tower. *Applied energy*, 127, 172-181. <https://doi.org/10.1016/j.apenergy.2014.04.031>
- Shen, C., & Li, X. (2017). Energy saving potential of pipe-embedded building envelope utilizing low-temperature hot water in the heating season. *Energy and buildings*, 138, 318-331. <https://doi.org/10.1016/j.enbuild.2016.12.064>
- Shen, C., Li, X., & Yan, S. (2017). Numerical study on energy efficiency and economy of a pipe-embedded glass envelope directly utilizing ground-source water for heating in diverse climates. *Energy Conversion and Management*, 150, 878-889. <https://doi.org/10.1016/j.enconman.2017.04.063>
- Shen, J., Wang, Z., Luo, Y., Jiang, X., Zhao, H., Cui, D. e., & Tian, Z. (2022). Performance evaluation of an active pipe-embedded building envelope system to transfer solar heat gain from the south to the north external wall. *Journal of Building Engineering*, 59, 105123. <https://doi.org/10.1016/j.jobbe.2022.105123>
- Su, X., Zhang, L., Liu, Z., Luo, Y., Lian, J., & Luo, Y. (2019). A computational model of an improved cooling radiant ceiling panel system for optimization and design. *Building and Environment*, 163, 106312. <https://doi.org/10.1016/j.buildenv.2019.106312>
- Sun, H., Wu, Y., Lin, B., Duan, M., Lin, Z., & Li, H. (2020). Experimental investigation on the thermal performance of a novel radiant heating and cooling terminal integrated with a flat heat pipe. *Energy and Buildings*, 208, 109646. <https://doi.org/10.1016/j.enbuild.2019.109646>
- Wang, L., Onn, C. C., Chew, B. T., Li, W., & Li, Y. (2024). Numerical Study of the Solar Energy-Powered Embedded Pipe Envelope System. *Buildings*, 14(3), 613. <https://doi.org/10.3390/buildings14030613>
- Xie, J.-l., Zhu, Q.-y., & Xu, X.-h. (2012). An active pipe-embedded building envelope for utilizing low-grade energy sources. *Journal of Central South University*, 19(6), 1663-1667. <https://doi.org/10.1007/s11771-012-1190-3>
- Xu, K., Xu, X., & Yan, T. (2023). Performance evaluation of a pipe-embedded phase change material (PE-PCM) roof integrated with solar collector. *Journal of Building Engineering*, 71, 106582. <https://doi.org/10.1016/j.jobbe.2023.106582>
- Xu, X., Wang, S., Wang, J., & Xiao, F. (2010). Active pipe-embedded structures in buildings for utilizing low-grade energy sources: a review. *Energy and buildings*, 42(10), 1567-1581. <https://doi.org/10.1016/j.enbuild.2010.05.002>
- Yang, M. (2014). Energy consumption analysis and energy-saving air conditioning technology application of commercial complexes in hot summer and cold winter regions Harbin Institute of Technology].
- Yang, Y., & Chen, S. (2024). Comprehensive thermal performances study on fin-enhanced thermo-activated building envelopes with anisotropic heat injection capacity. *Energy Conversion and Management*, 300, 117933. <https://doi.org/10.1016/j.enconman.2023.117933>
- Yang, Y., Chen, S., Chang, T., Ma, J., & Sun, Y. (2021). Uncertainty and global sensitivity analysis on thermal performances of pipe-embedded building envelope in the heating season. *Energy Conversion and Management*, 244, 114509. <https://doi.org/10.1016/j.enconman.2021.114509>
- Ye, M., Serageldin, A. A., Radwan, A., Sato, H., & Nagano, K. (2021). Thermal performance of ceiling radiant cooling panel with a segmented and concave surface: Laboratory analysis. *Applied Thermal Engineering*, 196, 117280. <https://doi.org/10.1016/j.applthermaleng.2021.117280>
- Yi, J. (2005). Energy consumption status of buildings in China and effective energy-saving methods. *Heating Ventilating & Air Conditioning*, 35(5), 11. <https://doi.org/10.3969/j.issn.1002-8501.2005.05.007>